# Bond-distance-dependent Auger decay of core-excited $N_2$ using an ultrashort x-ray pump and continuous-wave IR-control scheme

Qing Bian,[1] Yong Wu,[2,3] Jian Guo Wang,[2] and Song Bin Zhang[1,*]

[1]*School of Physics and Information Technology, Shaanxi Normal University, Xi'an 710119, China*

[2]*Institute of Applied Physics and Computational Mathematics, Beijing 100088, China*

[3]*Center for Applied Physics and Technology, Peking University, Beijing 100084, China*

(Received 4 January 2019; revised manuscript received 31 January 2019; published 5 March 2019)

Resonant Auger spectra (RAS) of core-excited $N_2$ are theoretically investigated by implementing an ultrashort x-ray pump and strong continuous-wave (CW) IR-control scheme. A femtosecond weak x-ray pump resonantly excites the nitrogen core-excited $1s \rightarrow \pi^*$ of the $N_2$ molecule; a strong CW IR control induces dynamic Stark shift of the core-excited level. With the pulse duration of the ultrashort pump comparable to or even shorter than the period of the IR control, the time overlapping between the pump and control pulses reduces into a subcycle of the IR pulse; the efficient pumping process strongly depends on the dynamic Stark shift and the relative phase between the two pulses, resulting in a great manipulation of the core-excited wave-packet dynamics and the subsequent RAS. The results are numerically illustrated for the $N_2$ molecule by a 2-fs x-ray pulse. The RAS also show a strong dependence on the bond-distance-dependent Auger decay probability.

DOI: 10.1103/PhysRevA.99.033404

## I. INTRODUCTION

With the development of the x-ray free-electron laser (FEL) facilities [1–6], it turns out to be possible to study the radiation-matter interaction under extreme conditions, such as unprecedented high intensities with the peak irradiance level up to $10^{18}$ W/cm$^2$ [7–10], and ultrashort pulse durations down to subfemtosecond [11–15]. With such a unique ultrashort and ultraintense x-ray FEL [16], Auger electron spectroscopy has burst into an increasing number of studies in atomic and molecular systems [17–27]. Taking only one ultrastrong pump pulse (maybe with a further weak probe pulse), both Rabi splitting and direct photoionization could also appear in the resonant Auger electron spectra (RAS), resulting in totally nonlinear RAS in the atomic and molecular cases [17,28–32]; the interference between Auger decay and direct photoionization and the light-induced nonadiabatic effect by the strong pump can totally distort the spectra [20,28,29,33–36]. However, with proper selections of the pulses, as shown in the recent works, these nonlinear Auger spectra can also be partially manipulated. Chatterjee and Nakajima [37] proposed the combination of strong resonant x-ray and nearly resonant optical pulses to investigate the effects of strong couplings in resonant Auger processes of the Ne atom; they showed that the shape of RAS can be changed by the intensities of the x-ray and/or optical pulses. Zhang *et al.* [38] proposed an all x-ray pump-control scheme for molecules, a weak pump creating the core-hole state and time-delayed strong control coupling the valance state and the core-hole state. The numerical results in the CO molecule were discussed and the core-excited vibrational dynamics and the subsequent Auger spectra can be efficiently manipulated by varying the time delays between the two pulses. In this work we proposed an alternative scheme to manipulate the RAS for a molecule with an ultrashort x-ray pump and CW IR control by the relative phase between the two pulses, using the advantages that the techniques of IR are very successful and the time synchronization between the pulses would be much easier to achieve; this scheme turns into a more practical candidate to be realized in FEL in the near future.

A prealigned $N_2$ molecule is chosen as the example to present this scheme, as shown in Fig. 1. The ultrashort and weak x-ray pump is executed within the CW IR pulse; Auger decay to the ionic state $|B\rangle$ is studied. The x-ray pump is chosen with central frequency $\omega_x = E_{|0\rangle_R} - E_{|0\rangle_I} = 400.88$ eV that it can resonantly excite the ground state $|0\rangle_I$ into the core-excited state $|0\rangle_R$ without the IR field. CW IR induces a dynamic Stark shift on the core-excited state $|R\rangle$, and it could alter the pumping process. Note that the core-excited system is a strong polar molecule with a big dipole moment, the peak intensity of the IR is supposed to be $\sim 10^{14}$ W/cm$^2$, and the Keldysh parameter [39] would be $\sim$0.1 or less. The multiphoton effect [40,41] can be assumed not significant [42]; tunneling ionization for high-harmonic generation (HHG) [43,44] is also weak and will not affect the present Auger process too much either. With IR intensity down to TW/cm$^2$, the Keldysh parameter would be $>1.0$, and we would expect important multiphoton effects, while the measurements can easily differentiate the electrons by their kinetic energies from different processes. With a proper selection of the pulse duration so that the ultrashort pump is comparable to or even shorter than the period of the IR control, the time overlapping between the pump and CW IR pulses reduces into a subcycle of the IR pulse, and the efficient pumping process will strongly depend on the dynamic Stark shift and the relative phase between the two pulses. As presented in the numerical results of prealigned $N_2$, the dynamics

*song-bin.zhang@snnu.edu.cn

 

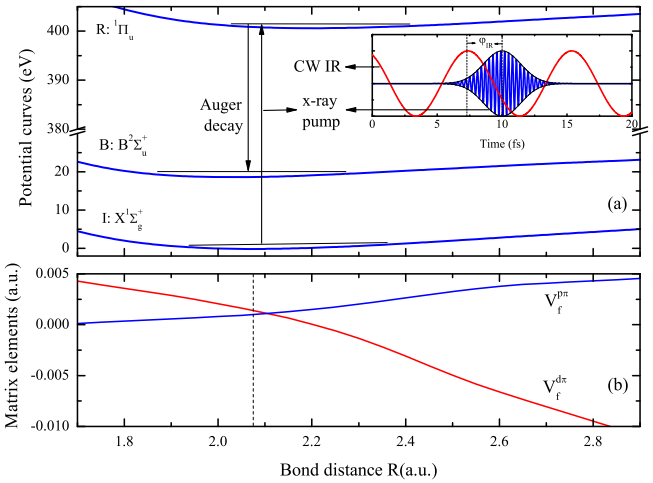


FIG. 1. Shown are the potential energy curves of the three involved electronic states (upper panel), and the bond-distance-dependent Coulomb matrix elements [45,46] $V^{p\pi/d\pi}(R)$ for the ionic state $B^2\Sigma_u^+$ (lower panel). The schematic of the x-ray pump and CW IR are illustrated in the inset of the upper panel.

of the core-excited wave packet and RAS can be efficiently manipulated by the CW IR pulse. Furthermore, Auger decay probabilities to the ionic state $|B\rangle$ show strong dependence on the nuclear bond distance [45,46], which is also carefully studied. The numerical method is briefly introduced in the next section together with the parameters used in the calculations, followed by a discussion of the numerical results in Sec. III and a conclusion in Sec. IV. Unless otherwise stated, atomic units (a.u.) are used throughout the paper.

## II. THEORETICAL METHODS

The time-dependent wave-packet propagation method [47–50] is applied to study the dynamics of the vibrational resolved RAS spectra by a pump-control scheme. Bearing in mind that three electronic states (the ground state $|I\rangle$, the core-excited state $|R\rangle$, and the final ionic state $|B\rangle$ with the electronic wave functions $\Phi_I$, $\Phi_R$, and $\Phi_B^\varepsilon$, respectively) are involved in the present study, within the Born-Oppenheimer approximation, the total wave function $\Psi(t)$ can be well expanded as

$$\Psi(t) = a_I(t)\Phi_I + a_R(t)e^{-i\omega t}\Phi_R + \int a_B^{p\pi}(\varepsilon,t)e^{-i\omega t}\Phi_B^\varepsilon d\varepsilon + \int a_B^{d\pi}(\varepsilon,t)e^{-i\omega t}\Phi_B^\varepsilon d\varepsilon, \tag{1}$$

where $a_I(t)$, $a_R(t)$, and $a_B^{p\pi/d\pi}(t)$ are the time-dependent amplitudes of the states $|I\rangle$, $|R\rangle$, and $|B\rangle$, respectively. $\varepsilon$ is Auger electron energy corresponding to the ionic state $|B\rangle$. The rapidly evolving phase factor $e^{-i\omega t}$ is explicitly separated, where $\omega$ is generally chosen to be the central frequency $\omega_x$ of the x-ray pump. By inserting the total wave function into the time-dependent Schrödinger equation, and implying the rotating wave approximation [51–53] and the local approximation [54,55], and supposing the laser pulses are much shorter than the molecular rotational period of $N_2$ and $N_2$ is prealigned, we can achieve the following working equations for the time-dependent amplitudes for a specific Auger electron energy $\varepsilon$ of aligned $N_2$ as

$$i\frac{\partial}{\partial t}\Phi(\varepsilon,t) = \hat{H}(R,t)\Phi(\varepsilon,t), \tag{2}$$

where

$$\Phi(\varepsilon,t) = \left[a_I(t) \quad a_R(t) \quad a_B^{p\pi}(\varepsilon,t) \quad a_B^{d\pi}(\varepsilon,t)\right]^T, \tag{3}$$

and

$$\hat{\mathrm{H}}(R,t) = \hat{\mathrm{T}}(R) + \begin{bmatrix} V_I(R) - \frac{i}{2}\Gamma_{ph}(t,t_0) & D_x^\dagger(t,t_0) & 0 & 0 \\ D_x(t,t_0) & V_R(R) - \frac{i}{2}\Gamma_{\mathrm{Aug}} - \omega_x - s_R(t,t_0,\varphi_{\mathrm{IR}}) & 0 & 0 \\ d_x^{p\pi}(t,t_0) & V^{p\pi}(R) & V_B(R) + \varepsilon - \omega_x & 0 \\ d_x^{d\pi}(t,t_0) & V^{d\pi}(R) & 0 & V_B(R) + \varepsilon - \omega_x \end{bmatrix}. \tag{4}$$

Here, $\hat{\mathrm{T}}(R)$ is the kinetic operator; $V_X(R)(X = I, R, B)$ is the potential energy curve of the corresponding electronic state $X$ (see Fig. 1); and the final ionic state $|B\rangle$ can be obtained by emitting electrons of $p\pi/d\pi$ via Coulomb matrix elements (Auger decay) $V^{p\pi/d\pi}(R)$ between the core-excited and final ionic state, or via direct photoionization $d_x^{p\pi/d\pi}(t,t_0) = d_{p\pi/d\pi}g_0 g(t,t_0)/2$ between the initial and final ionic states. $D_x(t,t_0) = d_{\mathrm{IR}}g_0 g(t,t_0)/2$ is the dipole coupling term between the ground and core-excited states; $\Gamma_{\mathrm{Aug}}$ is the total Auger decay width of the core-excited state; and $\Gamma_{ph}(t,t_0) = 2\pi[|d_x^{p\pi}(t,t_0)|^2 + |d_x^{d\pi}(t,t_0)|^2]$ stands for the leakage of the ground state caused by the direct photoionization. Note that multiphoton effect is weak in the present case; the theory of Eqs. (1)–(4) does not include channels to evaluate its effects. $d_{\mathrm{IR}}$ and $d_{p\pi/d\pi}$ are the dipole transition matrix elements; the Gaussian envelope $g(t,t_0) = e^{-(t-t_0)^2/\tau^2}$ with electric field intensity $g_0$, pulse duration $\tau$, and pulse center $t_0$ is employed in the calculations. $s_R(t,t_0,\varphi_{\mathrm{IR}}) = \Omega_R\cos[\omega_{\mathrm{IR}}(t-t_0)+\varphi_{\mathrm{IR}}]$ is the dynamic Stark shift on state $|R\rangle$, induced by the CW IR laser with center frequency $\omega_{\mathrm{IR}}$,

Rabi frequency $\Omega_R$, and phase $\varphi_{\rm IR}$ relative to the envelope peak of the pump pulse. Note that there is no permanent dipole or Stark shift for the ground state $|I\rangle$ of $N_2$. Finally the electron spectra pertaining to the ionic state $|B\rangle$ can be computed as the norm of the wave packet $\Phi_B(\varepsilon,t)$ at long times as

$$\sigma_B(\varepsilon) = \lim_{t\to\infty} \langle \Phi_B(\varepsilon,t) \mid \Phi_B(\varepsilon,t)\rangle. \tag{5}$$

In the present calculations, the three involved electronic states are modeled as Morse potentials with the spectroscopic constants from Refs. [45,46]. The bond-distance-dependent Coulomb matrix elements $V^{p\pi/d\pi}(R)$ from Refs. [45,46] shown in Fig. 1(b) for the ionic state $|B\rangle$ are employed; they are calculated within the framework of the one-center approximation describing the final states with a CI approach, and only two channels $lm$ with $p\pi$ and $d\pi$ symmetry contribute to the decay amplitudes [45,46]. The ratios between the transition dipoles are considered constant and optimized to best fit the synchrotron experimental RAS spectra [45,46] as $d_{p\pi}/d_{\rm IR} = 0.2$, $d_{d\pi}/d_{\rm IR} = 0.35$. Note that the Coulomb matrix elements at the equilibrium are $V^{p\pi}(R_e) = 0.001$ a.u. and $V^{d\pi}(R_e) = 0.0014$ a.u. The molecule is pumped by weak ultrashort x-ray laser pulses with $\tau = 2$ fs, Rabi frequency $\Omega_{\rm IR} = d_{\rm IR} g_0 = 0.0001$ a.u. and central frequency $\omega_x = E_{|0\rangle_R} - E_{|0\rangle_I} = 400.88$ eV, which resonantly excites the molecule from the ground state $|v=0\rangle_I$ to the core-excited state $|v=0\rangle_R$.

The vibrational energy spacing of state $|R\rangle$ is about 0.24 eV [45,46,56], much larger than the total Auger decay width $\Gamma_{\rm Aug} = 0.123$ eV [57] (decay lifetime of $1/\Gamma_{\rm Aug} = 5.35$ fs), so the lifetime vibrational interference (LVI) effect is not significant in the present case and the vibrational structures can be resolved from the Auger spectra. With such a short pump pulse of $\tau = 2$ fs, the pumping process strongly depends on both the pump pulse and the dynamic Stark shift of state $|R\rangle$; a quantity incorporating both the pump envelope and the structure of the CW IR dynamic Stark shift could be introduced as $s_R^e(t) = g(t,t_0)\cos[\omega_{\rm IR}(t-t_0)+\varphi_{\rm IR}]$. Only in the efficient region of $s_R^e(t) \neq 0$ do both the pump and CW IR pulses cooperate together. The bigger the $|s_R^e(t)|$, the stronger for both pumping and Stark shift; the positive and negative values of $s_R^e(t)$ indicate Stark lower and upper shifts of state $|R\rangle$, corresponding to the positive and negative off-resonant pumping of $|0\rangle_I \to |0\rangle_R$, respectively. The core-excited wave packet is totally related to the positive and negative oscillation structures of $s_R^e(t)$. In this work, we choose the typical IR so that when the relative phase $\varphi_{\rm IR} = 0$, the pumping can always excite more populations to $|v=1\rangle_R$ than the case without IR control. Such a pulse can be determined as mid-IR with wavelength $\lambda_{\rm IR} = 2\pi/\omega_{\rm IR} \geqslant 5\,\mu$m—only one broad peak structure for $s_R^e(t)$ or always positive off-resonant pumping of $|0\rangle_I \to |0\rangle_R$ in the whole efficient time region, and together with IR Rabi frequency $\Omega_R = 0.24$ eV. In the following work, $\lambda_{\rm IR} = 5\,\mu$m will be used as an example of CW IR to perform the numerical results with respect to different phases $\varphi_{\rm IR}$. The nuclear dynamics of Eqs. (2)–(5) is numerically solved by the well-known multiconfiguration time-dependent Hartree (MCTDH) [38] method.

Note that the mid-IR peak intensity required is assumed to be $\sim 10^{14}$ W/cm$^2$. For the mid-IR with pulse duration much longer than 2 fs (that of the ultrashort x-ray pump), for example, ~50 fs, such a mid-IR could be well considered as a "quasi" CW IR compared with the ultrashort x-ray pump. There are many reports of such lasers; for example, Wolter *et al.* [42] have reported 3.1 $\mu$m radiation with peak intensity $4\times10^{13}$ W/cm$^2$ and pulse duration of 71 fs, and von Grafenstein *et al.* [58] have reported 5-$\mu$m pulse with pulse duration of 160 fs and 7.7 GW peak power [if the laser focus was typically $(10\,\mu{\rm m})^2$, peak intensity would be $\sim 10^{14}$ W/cm$^2$]. The IR laser required should be experimentally achievable, at least in the near future.

## III. NUMERICAL RESULTS

Before presenting the numerical results of the pump-control scheme, RAS for only the weak pump pulse of $\omega_x = E_{|0\rangle_R} - E_{|0\rangle_I} = 400.88$ eV with respect to different pulse durations are studied and shown in Fig. 2. Both the effects of direct photoionization $[d_x^{p\pi/d\pi}(t)]$ and bond-distance-dependent Coulomb matrix elements $[V^{p\pi/d\pi}(R)]$ are included in the calculations. The spectra for long pulses ($\tau = 200$ fs) after convoluting the experimental resolution agree well with the synchrotron experimental results [45,46]. The spectra for different pulses are normalized to the main peak around 382.1 eV, corresponding to Auger electron energy from state $|0\rangle_R$ into state $|0\rangle_B$. Note that this peak is mainly contributed by direct photoionization [45,46]. This peak shows a blueshift from the energy $E_{|0\rangle_R} - E_{|0\rangle_B}$, due to the interference between Auger decay and direct photoionization (the peak is exactly at $E_{|0\rangle_R} - E_{|0\rangle_B}$ for calculations with only Auger decay or direct photoionization), and such an effect of blueshift is more significant for short pulses. With the decreasing of pulse duration, the spectra smear out the peaks and valleys and keep the main structures, but when $\tau$ is shorter than 20 fs, the vibrational period, new peak structures appear at the higher-energy region, which

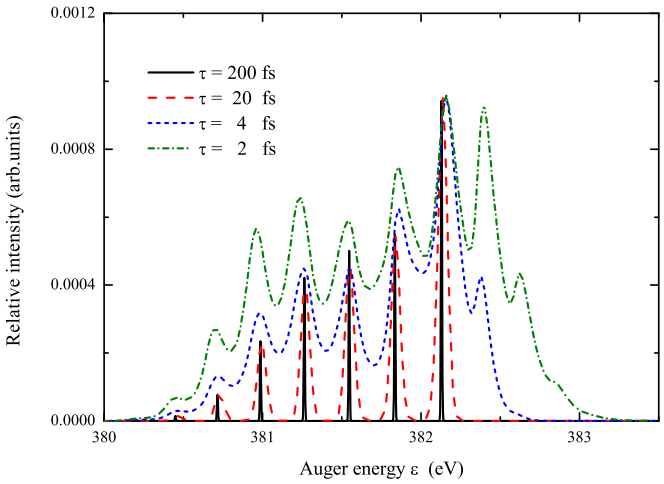


FIG. 2. Shown are RAS by resonant weak x-ray laser pulses with different pulse durations $\tau = 2$, 4, 20, and 200 fs, corresponding to ultrashort pulse, the lifetime of total Auger decay, the vibrational period of core-excited state, and very long pulse, respectively.

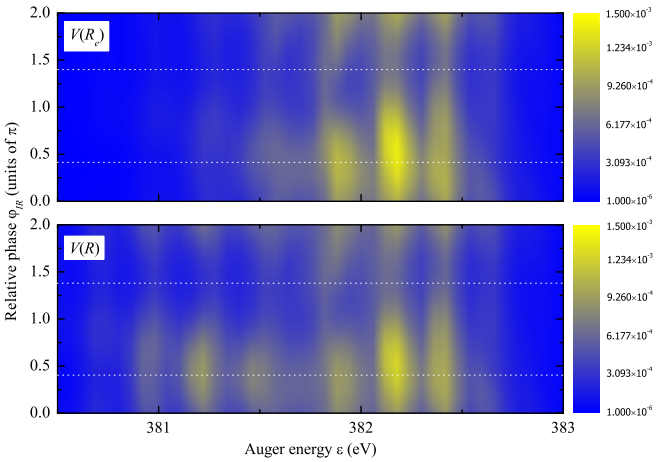


FIG. 3. Shown is the distribution of relative intensities of RAS as a function of the Auger electron energy $\varepsilon$ and the relative phase $\varphi_{\rm IR}$ between the two pulses. The effects of bond-distance-dependent probabilities are illustrated in different calculation models, $V^{p\pi/d\pi}(R)$ (lower panel) indicates the calculations with $R$-dependent Coulomb matrix elements, and $V^{p\pi/d\pi}(R_e)$ (upper panel) indicates the calculations with only the Coulomb matrix element at equilibrium position $R_e$.

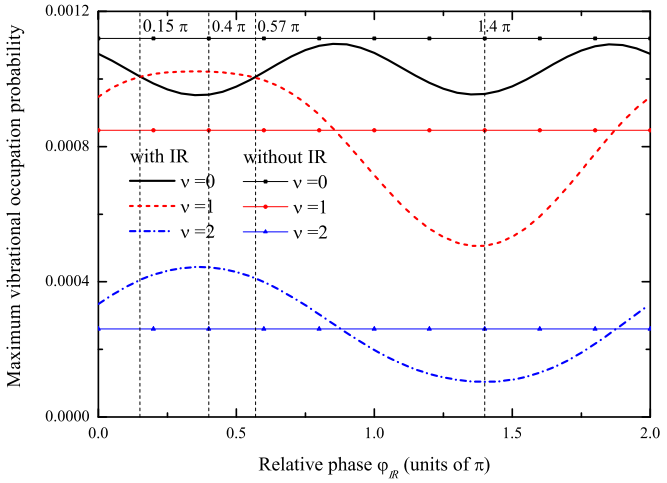


FIG. 4. Shown are the maximum values of vibrational occupation probabilities $p^m_{v=v_0}$ of the core-excited state with respect to the relative phase $\varphi_{\rm IR}$ between the two pulses.

comes from the fact that the bandwidths of such short pulses are bigger than the vibrational energy difference. The pump pulse with $\omega_x = E_{|0\rangle_R} - E_{|0\rangle_I}$ can also largely excite $|0\rangle_I$ into $|1, 2, ...\rangle_R$; subsequent Auger decays of $|1\rangle_R \to |0\rangle_B$, $|2\rangle_R \to |0\rangle_B$, and $|3\rangle_R \to |0\rangle_B$ reproduce the peaks around 382.4, 382.6, and 382.8 eV, respectively. Note that the anharmonicity of these three peaks is not significant, since $\omega_e\chi_e = 14.9\,{\rm cm}^{-1}$ for the core-excited state $|R\rangle$. With more vibrational states $|v\rangle_R$ excited, the peaks in the lower-energy region can be contributed by different decay channels; while the vibrational energy difference of state $|R\rangle$ is smaller than that of the final ionic state $|B\rangle$, these properties directly result into the small redshift of the peaks in the lower-energy region for ultrashort pulses. Furthermore, with more vibrational states $|v\rangle_R$ excited, the wave packet can evolve in a more broad region; bearing in mind that $|V^{p\pi/d\pi}(R)|$ is large for large $R$, their cooperated effect will enhance the Auger decay into the lower and higher regions, which is consistent with the features shown in Fig. 2—the relative intensities of the spectra at lower- and higher-energy regions become significant for short pulses.

Within the field of the CW IR pulse, RAS by the ultrashort x-ray pump can be totally changed. It is presented in the following with $\tau = 2\,{\rm fs}$ and $\lambda_{\rm IR} = 5\,\mu{\rm m}$ (see last section for details of the parameters) with respect to the relative phase $\varphi_{\rm IR}$, shown in Fig. 3. The effects of bond-distance-dependent probabilities are illustrated in the models $V^{p\pi/d\pi}(R)$ or $V^{p\pi/d\pi}(R_e)$, indicating calculations with $R$-dependent Coulomb matrix elements or only the values at equilibrium position $R_e$, respectively. As Fig. 3 shows, the electron spectra are very sensitive to the varying of phase $\varphi_{\rm IR}$, with $\varphi_{\rm IR}$ increasing from 0 to $2\pi$; the intensities of the whole spectra are enhanced to the "peak" and attenuated to the "valley" at about $\varphi_{\rm IR} = 0.4\pi$ and $1.4\pi$, respectively. The dynamic changes of the spectra to $\varphi_{\rm IR}$ should be directly related to the manipulation of the core-excited wave packet by the IR-control pulse through Stark shifts. The spectra for calculations in the models $V^{p\pi/d\pi}(R)$ or $V^{p\pi/d\pi}(R_e)$ are also very different, especially in the lower-energy region, indicating the important effects of bond-distance-dependent probabilities. Note that with $R$ displaced from $R_e$, $|V^{p\pi/d\pi}(R)|$ is generally larger than $|V^{p\pi/d\pi}(R_e)|$ [see Fig. 1(b)]; broad evolution of the core-excited wave packet would directly result in different results of the calculations with $V^{p\pi/d\pi}(R)$ or $V^{p\pi/d\pi}(R_e)$.

To get more insights on the effects on the core-excited wave packet by the control IR pulse, the vibrational occupation probabilities $p_v(t)$ of state $|R\rangle$ are studied for different $\varphi_{\rm IR}$. Excited from state $|I\rangle$ by the ultrashort ($\tau = 2\,{\rm fs}$) weak pump pulse, the occupation probability $p_{v=v_0}(t)$ increases to the maximum about 2 fs apart from the pump pulse, then decreases continuously due to Auger decay. The relative occupation probabilities for different vibrational states $v_0$ can be exhibited by the values of the maximums as $p^m_{v=v_0}$. As shown in Fig. 4, $p^m_{v=v_0}$ of state $|R\rangle$ depend strongly on the relative phase and experience oscillations with increasing of $\varphi_{\rm IR}$. Note that $p^m_{v=v_0}$ by only the same pump pulse are also labeled in the figure as dotted lines; they are 0.001 12, 0.000 85, and 0.000 26 for $v_0 = 0$, 1, and 2, respectively. Within the field of the IR-control pulse, state $|R\rangle$ is shifted by the dynamic Stark shifts, or the core-excited state is dressed as $|\widetilde{R}\rangle$; the resonant frequency $\omega_x = E_{|0\rangle_R} - E_{|0\rangle_I} = 400.88\,{\rm eV}$ for state $|R\rangle$ will surely displace from the resonant one $E_{|0\rangle_{\widetilde{R}}} - E_{|0\rangle_I}$ for the dressed state $|\widetilde{R}\rangle$, resulting in $p^m_{v=0}$ being always a little smaller than 0.001 12. The variations of $p^m_{v=0}$ are only within $\sim$10% for different $\varphi_{\rm IR}$. When $\varphi_{\rm IR} \approx 0$ (or $\pi$), state $|R\rangle$ is negatively (or positively) shifted during the whole pumping process, $\omega_x = E_{|0\rangle_R} - E_{|0\rangle_I}$ becomes close to (or far away from) the resonant frequencies $E_{|1\rangle_{\widetilde{R}}} - E_{|0\rangle_I}$ and $E_{|2\rangle_{\widetilde{R}}} - E_{|0\rangle_I}$; $p^m_{v=1}$ and $p^m_{v=2}$ will simultaneously increase (or decrease) in contrast to the case without IR control. Note that when $\varphi_{\rm IR}$ are far from 0 and $\pi$, $s^e_R(t)$ could be positive and negative in the pumping field; the changes of $p^m_{v=1,2}$ cannot be easily predicted. As it also shows, $p^m_{v=1,2}$ experience the similar "up-down-up" structure with the increasing of $\varphi_{\rm IR}$, and they

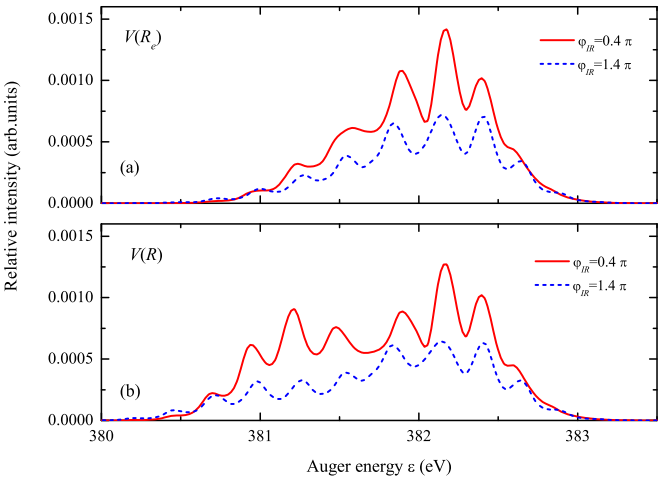


FIG. 5. Shown are the typical RAS in models $V^{p\pi/d\pi}(R_e)$ (upper panel) and $V^{p\pi/d\pi}(R)$ (lower panel) for the cases with relative phase $\varphi_{\rm IR} = 0.4\pi$ and $\varphi_{\rm IR} = 1.4\pi$, corresponding to the spectra peak and valley shown in Fig. 3, respectively.

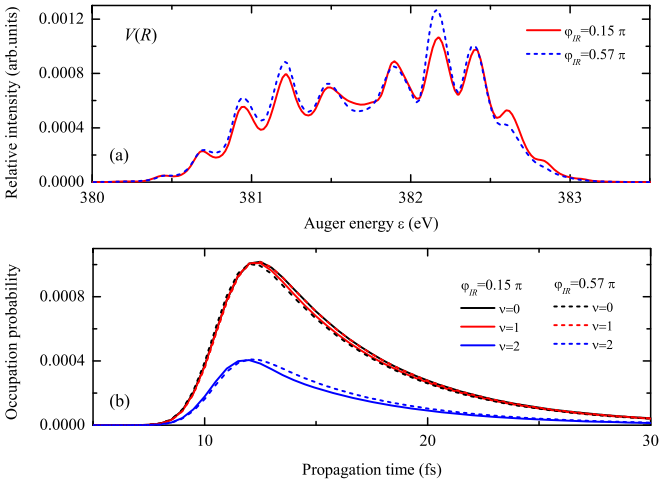


FIG. 6. Shown are the typical RAS [model $V^{p\pi/d\pi}(R)$] for the cases with relative phase $\varphi_{\rm IR} = 0.15\pi$ and $\varphi_{\rm IR} = 0.57\pi$ (upper panel), and the time-dependent vibrational occupation probabilities (lower panel); the ultrashort x-ray pulse is centered at 10 fs.

change very significantly for different $\varphi_{\rm IR}$; the ratios between the peak (at $\varphi_{\rm IR} \approx 0.4\pi$) and valley (at $\varphi_{\rm IR} \approx 1.4\pi$) of $p^m_{v=1}$ and $p^m_{v=2}$ are about two and three times, respectively. Bearing in mind that $p^m_{v=0}$ and $p^m_{v=1}$ are comparable for $0 < \varphi_{\rm IR} < \pi$, and $p^m_{v=0}$ do not vary too much while $p^m_{v=1}$ vary a lot for different $\varphi_{\rm IR}$, and $p^m_{v=0,1}$ are much larger than $p^m_{v=2}$ for different $\varphi_{\rm IR}$, the intensities of the electron spectra with respect to $\varphi_{\rm IR}$ would strongly depend on the variations of $p^m_{v=1}$ with respect to $\varphi_{\rm IR}$, which is consistent with the features revealed in Fig. 3 for the electron spectra; i.e., both the electron spectra and $p^m_{v=1}$ increase up to the peak until $\varphi_{\rm IR} \approx 0.4\pi$, then continuously decease down to the valley until $\varphi_{\rm IR} \approx 1.4\pi$, and finally increase until $\varphi_{\rm IR} \approx 2\pi$. Note that the x-ray pump is weak; the excitations to different $|v\rangle_R$ should couple very weakly with each other. The dynamics and oscillation periods of $p^m_{v=1,2,3}$ with respect to $\varphi_{\rm IR}$ could be directly related to the x-ray frequency and the geometric properties of $s^e_R(t)$.

The typical electron spectra for the spectra peak and valley are shown in Fig. 5, corresponding to $\varphi_{\rm IR} = 0.4\pi$ and $1.4\pi$, respectively. The spectra intensities of $\varphi_{\rm IR} = 0.4\pi$ are about two times stronger than that of $\varphi_{\rm IR} = 1.4\pi$, which are mainly determined by different pumping excitations in the IR-control field [$p^m_{v=0}(\varphi_{\rm IR} = 0.4\pi) \simeq p^m_{v=0}(\varphi_{\rm IR} = 1.4\pi)$, $p^m_{v=1}(\varphi_{\rm IR} = 0.4\pi) \simeq 2 \times p^m_{v=1}(\varphi_{\rm IR} = 1.4\pi)$]. Note that interference from different channels should exhibit effects in the spectra; while the results show that the ratios of changes for the spectra intensities and the vibrational populations ($p^m_{v=1}$) are very similar, it indicates the interference effect is not so significant in the present case. The spectra in the models $V^{p\pi/d\pi}(R)$ and $V^{p\pi/d\pi}(R_e)$ are very similar for $\varphi_{\rm IR} = 1.4\pi$, but differ a lot for $\varphi_{\rm IR} = 0.4\pi$ in the lower-energy region, which can be easily understood from the cooperation of $p_v(t)$ and the $R$-dependent Coulomb matrix elements $V^{p\pi/d\pi}(R)$; i.e., when $\varphi_{\rm IR} = 1.4\pi$, $p_{v=0}(t)$ dominates the occupation probabilities in state $|R\rangle$ ($p^m_{v=0} \gg p^m_{v=1,2}$), the core-excited wave packet mainly evolves in the small spatial region around $R_e$, and the spectra in models $V^{p\pi/d\pi}(R)$ and $V^{p\pi/d\pi}(R_e)$ will surely be similar. When $\varphi_{\rm IR} = 0.4\pi$, the excitation to $|v = 1\rangle_R$ dominates the core-excited wave packet; let us bear in mind that the Franck Condon region from the $|v = 1\rangle_R$ to the state $|v'\rangle_B$ locates mainly in the lower-energy region, and Auger decay with more wave packets from $|v = 1\rangle_R$ will surely enhance the spectra in the lower-energy region. The spectra differences of the model $V^{p\pi/d\pi}(R_e)$ shown in Fig. 5(a) below 382 eV should be mainly attributed to this effect. In addition, the spatial density distribution of $|v = 1\rangle_R$ is much broader than that of $|v = 0\rangle_R$ in the small spatial region around $R_e$; note that $|V^{p\pi/d\pi}(R)|$ is much bigger than $|V^{p\pi/d\pi}(R_e)|$ in the region far away from $R_e$, and the spectra in the lower-energy region will be further and significantly enhanced by Auger decay with more wave packets from the state $|v = 1\rangle_R$. Such an effect mainly results in the big differences of the spectra of the models $V^{p\pi/d\pi}(R)$ and $V^{p\pi/d\pi}(R_e)$ for $\varphi_{\rm IR} = 0.4\pi$ below 382 eV shown in Fig. 5.

Figure 6(a) shows the typical spectra for $\varphi_{\rm IR} = 0.15\pi$ and $0.57\pi$ with the "same" $p^m_{v=0,1,2}$. As it shows, the spectra of these two cases are also quite different, although the occupation probabilities for each vibrational states are almost the same [see Fig. 6(b) for the occupation probabilities for different vibrational states]. It indicates the phases induced by the present pump-control scheme for the vibrational states of these two cases are different, and such phases also play important roles in the Auger electron spectra.

## IV. CONCLUSIONS

The scheme of ultrashort x-ray pump and CW IR control is proposed to study resonant Auger spectra (RAS) of core-excited $N_2$. A femtosecond x-ray pump resonantly excites the nitrogen core-excited $1s \rightarrow \pi^*$ of the $N_2$ molecule within the field of a CW IR-control pulse, which induces dynamic Stark shift of the core-excited level and changes the pumping excitations. With the pulse duration of the ultrashort pump comparable to or even shorter than the period of the IR control, the time overlapping between the pump and control pulses reduces into a subcycle of the IR pulse, and the efficient

pumping process strongly depends on not only the dynamic Stark shift but also the relative phase $\varphi_{\mathrm{IR}}$ between the two pulses, resulting in a great manipulation of the core-excited wave-packet dynamics and the subsequent RAS. The results are numerically illustrated for a $N_2$ molecule by a 2-fs x-ray pulse with $\omega_x = E_{|0\rangle_R} - E_{|0\rangle_I} = 400.88\,\mathrm{eV}$ and an IR pulse with $\lambda_{\mathrm{IR}} = 5\,\mu\mathrm{m}$. It shows the spectra depend strongly on the relative phase $\varphi_{\mathrm{IR}}$, and the spectra variations with respect to $\varphi_{\mathrm{IR}}$ are mainly determined by the relative occupation probabilities of the vibrational state $|v = 1\rangle_R$. RAS also show a strong dependence on the bond-distance-dependent Auger decay probability.

## ACKNOWLEDGMENTS

Grants from the National Basic Research Program of China (Grant No. 2017YFA0403200), NSFC (Grant No. 11604197), the Science Challenge Program of China (Grants No. TZ2018005 and No. TZ2016005), and the Organization Department of CCCPC are acknowledged.

[1] L.-H. Yu, M. Babzien, I. Ben-Zvi, L. F. DiMauro, A. Doyuran, W. Graves, E. Johnson, S. Krinsky, R. Malone, I. Pogorelsky *et al.*, Science **289**, 932 (2000).
[2] K. Tiedtke, A. Azima, N. v. Bargen, L. Bittner, S. Bonfigt, S. Düsterer, B. Faatz, U. Frühling, M. Gensch, G. Ch *et al.*, New J. Phys. **11**, 023029 (2009).
[3] E. Allaria, C. Callegari, D. Cocco, W. M. Fawley, M. Kiskinova, C. Masciovecchio, and F. Parmigiani, New J. Phys. **12**, 075002 (2010).
[4] P. Emma, R. Akre, J. Arthur, R. Bionta, C. Bostedt, J. Bozek, A. Brachmann, P. Bucksbaum, R. Coffee, F. J. Decker *et al.*, Nat. Photon. **4**, 641 (2010).
[5] T. Ishikawa, H. Aoyagi, T. Asaka, Y. Asano, N. Azumi, T. Bizen, H. Ego, K. Fukami, T. Fukui, Y. Furukawa *et al.*, Nat. Photon. **6**, 540 (2012).
[6] C. Bostedt, S. Boutet, D. M. Fritz, Z. Huang, H. J. Lee, H. T. Lemke, A. Robert, W. F. Schlotter, J. J. Turner, and G. J. Williams, Rev. Mod. Phys. **88**, 015007 (2016).
[7] L. Young, E. P. Kanter, B. Krässig, Y. Li, A. M. March, S. T. Pratt, R. Santra, S. H. Southworth, N. Rohringer, L. F. DiMauro *et al.*, Nature **466**, 56 (2010).
[8] E. Allaria, F. Bencivenga, R. Borghes, F. Capotondi, D. Castronovo, P. Charalambous, P. Cinquegrana, M. B. Danailov, G. De Ninno, A. Demidovich *et al.*, Nat. Commun. **4**, 2476 (2013).
[9] A. Marinelli, D. Ratner, A. A. Lutman, J. Turner, J. Welch, F.-J. Decker, H. Loos, C. Behrens, S. Gilevich, A. A. Miahnahri *et al.*, Nat. Commun. **6**, 6369 (2015).
[10] J. Szlachetko, J. Hoszowska, J.-C. Dousse, M. Nachtegaal, W. Blachucki, Y. Kayser, J. Sà, M. Messerschmidt, S. Boutet, G. J. Williams *et al.*, Sci. Rep. **6**, 33292 (2016).
[11] A. A. Lutman, R. Coffee, Y. Ding, Z. Huang, J. Krzywinski, T. Maxwell, M. Messerschmidt, and H.-D. Nuhn, Phys. Rev. Lett. **110**, 134801 (2013).
[12] N. Hartmann, W. Helml, A. Galler, M. R. Bionta, J. Grünert, S. L. Molodtsov, K. R. Ferguson, S. Schorb, M. L. Swiggers, S. Carron *et al.*, Nat. Photon. **8**, 706 (2014).
[13] W. Helml, A. R. Maier, W. Schweinberger, I. Grguraš, P. Radcliffe, G. Doumy, C. Roedig, J. Gagnon, M. Messerschmidt, S. Schorb *et al.*, Nat. Photon. **8**, 950 (2014).
[14] J. Maxson, D. Cesar, G. Calmasini, A. Ody, P. Musumeci, and D. Alesini, Phys. Rev. Lett. **118**, 154802 (2017).
[15] P. Emma, K. Bane, M. Cornacchia, Z. Huang, H. Schlarb, G. Stupakov, and D. Walz, Phys. Rev. Lett. **92**, 074801 (2004).
[16] J. Ullrich, A. Rudenko, and R. Moshammer, Annu. Rev. Phys. Chem. **63**, 635 (2012).
[17] N. Rohringer and R. Santra, Phys. Rev. A **77**, 053404 (2008).
[18] J.-C. Liu, Y.-P. Sun, C.-K. Wang, H. Ågren, and F. Gel'mukhanov, Phys. Rev. A **81**, 043412 (2010).
[19] E. P. Kanter, B. Krässig, Y. Li, A. M. March, P. Ho, N. Rohringer, R. Santra, S. H. Southworth, L. F. DiMauro, G. Doumy *et al.*, Phys. Rev. Lett. **107**, 233001 (2011).
[20] P. V. Demekhin, Y.-C. Chiang, and L. S. Cederbaum, Phys. Rev. A **84**, 033417 (2011).
[21] N. Rohringer and R. Santra, Phys. Rev. A **86**, 043434 (2012).
[22] V. Kimberg, S. B. Zhang, and N. Rohringer, J. Phys. B **46**, 164017 (2013).
[23] B. K. McFarland, J. P. Farrell, S. Miyabe, F. Tarantelli, A. Aguilar, N. Berrah, C. Bostedt, J. D. Bozek, P. H. Bucksbaum, J. C. Castagna *et al.*, Nat. Commun. **5**, 4235 (2014).
[24] S. B. Zhang and N. Rohringer, Phys. Rev. A **89**, 013407 (2014).
[25] A. D. Müller and P. V. Demekhin, J. Phys. B **48**, 075602 (2015).
[26] S. B. Zhang and N. Rohringer, Phys. Rev. A **92**, 043420 (2015).
[27] S. B. Zhang, X. T. Xie, and J. G. Wang, Phys. Rev. A **96**, 053420 (2017).
[28] L. S. Cederbaum, Y.-C. Chiang, P. V. Demekhin, and N. Moiseyev, Phys. Rev. Lett. **106**, 123001 (2011).
[29] P. V. Demekhin and L. S. Cederbaum, Phys. Rev. A **83**, 023422 (2011).
[30] B. M. Lagutin, I. D. Petrov, V. L. Sukhorukov, S. Kammer, S. Mickat, R. Schill, K.-H. Schartner, A. Ehresmann, Y. A. Shutov, and H. Schmoranzer, Phys. Rev. Lett. **90**, 073001 (2003).
[31] B. M. Lagutin, I. D. Petrov, V. L. Sukhorukov, Ph V. Demekhin, B. Zimmermann, S. Mickat, S. Kammer, K.-H. Schartner, A. Ehresmann, Yu A. Shutov *et al.*, J. Phys. B **36**, 3251 (2003).
[32] E. Kukk, J. D. Bozek, W.-T. Cheng, R. F. Fink, A. A. Wills, and N. Berrah, J. Chem. Phys. **111**, 9642 (1999).
[33] M. Šindelka, N. Moiseyev, and L. S. Cederbaum, J. Phys. B **44**, 045603 (2011).
[34] G. J. Halász, Á. Vibók, N. Moiseyev and L. S. Cederbaum, J. Phys. B **45**, 135101 (2012).
[35] P. V. Demekhin and L. S. Cederbaum, J. Phys. B **46**, 164008 (2013).
[36] N. Moiseyev and M. Šindelka, J. Phys. B **44**, 111002 (2011).
[37] S. Chatterjee and T. Nakajima, Phys. Rev. A **91**, 043413 (2015).
[38] S. B. Zhang, V. Kimberg, and N. Rohringer, Phys. Rev. A **94**, 063413 (2016).
[39] L. V. Keldysh, Sov. Phys. JETP **20**, 1307 (1965).
[40] J. E. Bayfield and P. M. Koch, Phys. Rev. Lett. **33**, 258 (1974).
[41] E. J. Galvez, B. E. Sauer, L. Moorman, P. M. Koch, and D. Richards, Phys. Rev. Lett. **61**, 2011 (1988).

[42] B. Wolter, M. G. Pullen, M. Baudisch, M. Sclafani, M. Hemmer, A. Senftleben, C. D. Schröter, J. Ullrich, R. Moshammer, and J. Biegert, Phys. Rev. X **5**, 021034 (2015).
[43] J. L. Krause, K. J. Schafer, and K. C. Kulander, Phys. Rev. Lett. **68**, 3535 (1992).
[44] P. B. Corkum, Phys. Rev. Lett. **71**, 1994 (1993).
[45] M. N. Piancastelli, R. F. Fink, R. Feifel, M. Bässler, S. L. Sorensen, C. Miron, H. Wang, I. Hjelte, O. Björneholm, A. Ausmees *et al.*, J. Phys. B **33**, 1819 (2000).
[46] P. Sałek, R. F. Fink, F. Gel'mukhanov, M. N. Piancastelli, R. Feifer, M. Bässler, S. L. Sorensen, C. Miron, H. Wang, I. Hjelte *et al.*, Phys. Rev. A **62**, 062506 (2000).
[47] L. S. Cederbaum and F. Tarantelli, J. Chem. Phys. **99**, 5871 (1993).
[48] E. Pahl, H. D. Meyer, and L. S. Cederbaum, Z. Phys. D **38**, 215 (1996).
[49] E. Pahl, J. Brand, L. S. Cederbaum, and F. Tarantelli, Phys. Rev. A **60**, 1079 (1999).
[50] L. S. Cederbaum and F. Tarantelli, J. Chem. Phys. **98**, 9691 (1993).
[51] G. S. Agarwal, Phys. Rev. A **4**, 1778 (1971).
[52] K. Zaheer and M. S. Zubairy, Phys. Rev. A **37**, 1628 (1988).
[53] A. Brown, W. J. Meath, and P. Tran, Phys. Rev. A **63**, 013403 (2000).
[54] W. Domcke, Phys. Rep. **208**, 97 (1991).
[55] L. S. Cederbaum and W. Domcke, J. Phys. B **14**, 4665 (1981).
[56] J. E. Rubensson, M. Neeb, M. Biermann, Z. Xu, and W. Eberhardt, J. Chem. Phys. **99**, 1633 (1993).
[57] C. T. Chen, Y. Ma, and F. Sette, Phys. Rev. A **40**, 6737 (1989).
[58] L. von Grafenstein, M. Bock, D. Ueberschaer, K. Zawilski, P. Schunemann, U. Griebner, and T. Elsaesser, Opt. Lett. **42**, 3796 (2017).